

# A macro-tidal freshwater ecosystem recovering from hypereutrophication: the Schelde case study

T. J. S. Cox<sup>1,2</sup>, T. Maris<sup>1</sup>, K. Soetaert<sup>2</sup>, D. J. Conley<sup>3</sup>, S. Van Damme<sup>1</sup>, P. Meire<sup>1</sup>, J. J. Middelburg<sup>2</sup>, M. Vos<sup>2,4</sup>, and E. Struyf<sup>1,3</sup>

<sup>1</sup>University of Antwerp, Department of Biology, Ecosystem Management research group, Universiteitsplein 1, 2610 Anwerpen, Belgium

<sup>2</sup>Netherlands Institute of Ecology (NIOO-KNAW), Centre for Estuarine and Marine Ecology, Korrिंगaweg 7, P.O. Box 140, 4400 AC Yerseke, The Netherlands

<sup>3</sup>GeoBiosphere Science Centre, Quaternary Sciences, Sölvegatan 12, 223 62 Lund, Sweden

<sup>4</sup>University of Potsdam, Institute of Biochemistry and Biology, Dept. Ecology & Ecosystem Modeling, Am Neuen Palais 10, 14469 Potsdam, Germany

Received: 7 May 2009 – Published in Biogeosciences Discuss.: 3 June 2009

Revised: 30 November 2009 – Accepted: 5 December 2009 – Published: 10 December 2009

**Abstract.** We report a 40 year record of eutrophication and hypoxia on an estuarine ecosystem and its recovery from hypereutrophication. After decades of high inorganic nutrient concentrations and recurring anoxia and hypoxia, we observe a paradoxical increase in chlorophyll-*a* concentrations with decreasing nutrient inputs. We hypothesise that algal growth was inhibited due to hypereutrophication, either by elevated ammonium concentrations, severe hypoxia or the production of harmful substances in such a reduced environment. We study the dynamics of a simple but realistic mathematical model, incorporating the assumption of algal growth inhibition. It shows a high algal biomass, net oxygen production equilibrium with low ammonia inputs, and a low algal biomass, net oxygen consumption equilibrium with high ammonia inputs. At intermediate ammonia inputs it displays two alternative stable states. Although not intentional, the numerical output of this model corresponds to observations, giving extra support for assumption of algal growth inhibition. Due to potential algal growth inhibition, the recovery of hypereutrophied systems towards a classical eutrophied state, will need reduction of waste loads below certain thresholds and will be accompanied by large fluctuations in oxygen concentrations. We conclude that also flow-through systems, heavily influenced by external forcings which partly mask internal system dynamics, can display multiple stable states.

## 1 Introduction

Low oxygen concentrations and harmful phytoplankton blooms are among the most severe human-induced impacts on surface waters. The degradation of allochthonous organic matter by heterotrophic organisms made large bodies of water hypoxic, sometimes anoxic, and over-saturated with carbon dioxide (Vandijk et al., 1994; Heip et al., 1995; Frankignoulle et al., 1998). Increased nutrient loads enhanced autochthonous production, resulting in harmful algal blooms and bottom water hypoxia events (Carpenter et al., 1998; Smith, 2003; Diaz and Rosenberg, 2008; Kemp et al., 2009).

The response of aquatic systems to changes in nutrient and organic matter load can be far from gradual, and instead may reveal rich, non-linear dynamics. Most famous in this respect are shallow lakes, which have become textbook examples of ecosystems that can suddenly shift between alternative states (Carpenter et al., 1999; Scheffer et al., 2001). Eutrophied coastal systems have also been suggested to show hysteresis, regime shifts and pollution thresholds (Petersen et al., 2008; Duarte et al., 2009; Conley et al., 2009), as is the Black Sea (Oguz and Gilbert, 2007). In flow-through systems, such as rivers and estuaries, the potential for non-linear dynamics received far less attention, mainly because of the assumption that their biogeochemistry is controlled by physical forcing (flow rate, mixing processes, light availability, wind speed) rather than by internal, biological processes (Dent et al., 2002). Nevertheless, biological control of biogeochemistry is in some cases as important as physical forcing (e.g. Strayer et al., 2008).



Correspondence to: T. J. S. Cox  
(tom.cox@ua.ac.be)

Here we study the dynamics of the freshwater reach of a well documented, highly eutrophied estuary (Schelde, Belgium), in which nitrification and bacterial breakdown of allochthonous organic matter has caused severe hypoxia and anoxia. This resulted in a far more degraded situation than many other systems affected by eutrophication. With reductions in waste loads, a recovery of the brackish and saline estuarine reaches has been witnessed over the last two decades (Soetaert et al., 2006). From a 40 year combined data set we demonstrate that also the freshwater reach is now recovering. A paradoxical increase in chlorophyll-*a* concentrations with decreasing nutrient inputs is observed, suggesting that primary production was until recently inhibited in this hyper-eutrophic system. On basis of this information we develop a simple but realistic mathematical model incorporating the assumption that low oxygen concentrations negatively affect algal growth, and compare its output with the observed data. We argue that during its recovery from hypereutrophication, the freshwater Schelde, might have gone through period with two alternative stable states. This transition from hypereutrophication to a classical eutrophied state needs reduction of waste loads below a defined threshold, and is marked by large fluctuations in oxygen concentration.

## 2 Material and methods

### 2.1 Site description

The Schelde estuary is situated in Northern Belgium (Flanders) and the Southwest of The Netherlands. The total area draining into the estuary is about 22 000 km<sup>2</sup>. The tidal wave enters deeply inland, resulting in about 240 km of estuarine reaches experiencing a macro tidal regime. The estuary exhibits the unique transition from salt over brackish to freshwater tidal areas (Meire et al., 2005). Weirs blocking the tidal wave determine the upstream boundaries of the estuary. Following Elliott and McLusky (2002) we define the freshwater tidal reach (FW) as that part of the estuary with salinity < 0.5. The focus of our study is the 35 km freshwater stretch of the main branch of the estuary (Fig. 1). The average tidal range in this stretch is about 3 m.

Water column biogeochemistry in this part of the estuary is largely determined by pelagic processes. The sediments of the main channel are biologically and chemically quasi inert. Due to high turbidity, benthic primary production in the river bed (minimum water column depth is 3 m) is excluded. The strong dynamics of overflowing water keeps most particles permanently in suspension and therefore limits the downward flux of organic matter. For the same reason there are no vascular plants growing in the main channel and benthic organisms are virtually absent. Due to embankments, the area of intertidal flats and marshes has been decimated, excluding a significant impact to water column biogeochemistry from there (Meire et al., 2005; Van Damme et al., 2005). In con-

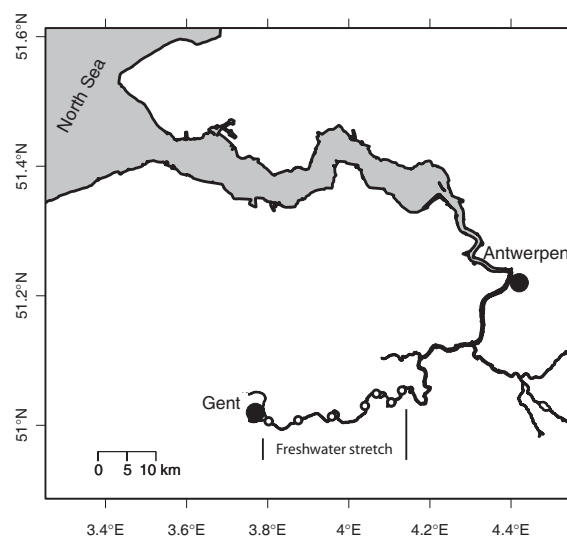


**Fig. 1.** The Schelde-estuary upto the weirs blocking the tidal wave and determining the upstream boundaries. The OMES monitoring stations (1995-present) in the 35 km freshwater tidal stretch are marked with a circle.

trast, the Westerschelde (the brackish and saline part of the estuary) has large tidal flats. But even there, microphyto-benthos production for example, has been estimated to account for less than 17% of total algal production (de Jong and De Jonge, 1995; Heip et al., 1995; Kromkamp et al., 1995). As in other temperate tidal estuaries, when compared to pelagic processes the role of benthic processes on pelagic biogeochemistry is of minor importance on the ecosystem scale (Heip et al., 1995; Soetaert and Herman, 1995b; Vanderborgh et al., 2007). Macro-algae do not play a significant role in turbid, tidal estuaries and are absent in our system (Heip et al., 1995).

Agricultural, urban and industrial pressures, resulted in a notorious history of pollution, eutrophication and habitat degradation of the Schelde estuary (Wollast, 1988; Meire et al., 2005; Van Damme et al., 2005; Soetaert et al., 2006), and caused changes in the food-web structure and overall carbon cycling of the adjacent coastal zone, the Southern Bight of the North Sea (Lancelot et al., 2005, 2007; Gypens et al., 2009). Organic pollution and associated bacterial activity made a large part of the estuary hypoxic, with some parts permanently hypoxic and seasonally anoxic. Nitrification is generally quoted as the major process leading to suboxic conditions in eutrophic, turbid estuaries (Heip et al., 1995). The high observed nitrification rates in maximum turbidity zones are explained by the attachment of nitrifiers to particles, increasing their retention time and allowing them to attain high biomass (Owens, 1986). Until the early 2000s, nitrification was the major oxygen consuming process in the freshwater Schelde. Unpublished oxygen uptake experiments with and without nitrification inhibitors on the freshwater Schelde

for the 1998–2003 period, show that on average nitrification in this part of the estuary accounts for 50% of total oxygen consumption, with maxima of 75%. Schuchardt et al. (1993) reported similar values in the freshwater reach of the Weser estuary (Germany). Research on the brackish and saline parts of the Schelde estuary confirms that nitrification rates are highest in the most upstream parts, and show a declining long term trend of relative contribution to total oxygen demand (Billen G, 1975; Somville, 1984; Gazeau et al., 2005). Compared to other estuaries, the observed nitrification rates in the (freshwater) Schelde are extremely high (Somville, 1984; de Bie et al., 2002). Therefore, nitrification has received major attention in all ecosystem modelling studies of the Schelde (Billen et al., 1985; Soetaert and Herman, 1995a,b; Billen et al., 2005; Vanderborght et al., 2002, 2007; Hofmann et al., 2008).

Before 1996 the water quality of the Schelde freshwater tidal reaches was not systematically monitored. The data presented in this manuscript are compiled from a variety of sources. Data for 1967–1969 are taken from the PhD dissertation of De Pauw (1975). Between 1975 and 1983 several sampling cruises were undertaken, coordinated at the Université Libre de Bruxelles (ULB) (Billen et al., 1985; Wollast, 1988). From 1977 to 1991 the Belgian Institute for Hygiene and Epidemiology (IHE) analysed a limited number of water samples every year. In 1989 a few cruises conducted by the Netherlands Institute of Ecology (NIOO-CEME) reached into the freshwater reach. Data between 1989 and 1993 were collected by the Flemish Environmental Agency (VMM). Beginning in 1996 the freshwater tidal reaches of the Schelde estuary were included in a systematic, long term monitoring campaign (OMES), coordinated at the University of Antwerp (Van Damme et al., 2005). Table 1 presents for each year the data sources and the number of available data points.

## 2.2 Numerical modelling

All numerical analyses were performed in *R* ([www.r-project.org](http://www.r-project.org)). Model integration and calculation of steady state solutions were performed with *R*-packages *deSolve* and *rootSolve* available from CRAN (Soetaert and Herman, 2009). Stable states were determined by running the model to steady state from different initial conditions. Unstable equilibrium points were determined manually by iteratively reducing the searched part of state space. The range of the different state variables was progressively decreased, 10 000 random state variables were generated in this range and the time derivative of the state variables at these points was calculated. When this time derivative is zero, the system is in (stable or unstable) equilibrium.

## 3 Results

### 3.1 Water quality in the FW Schelde from the 1960s to present

Although data for the period 1968–1995 are obtained from different sources and show considerable spatial, inter- and intra-annual variability, a clear pattern emerges in the annual, FW averages (Fig. 2; the annual, FW average is calculated by averaging over all stations in the FW reach for each year). Average total ammonium concentrations (the sum of  $\text{NH}_4^+$  and  $\text{NH}_3$  concentration, hereafter referred to as ammonium) were high, typically between 250 and  $1000 \mu\text{mol L}^{-1}$ ; also average dissolved inorganic phosphorus (DIP) concentrations were high, typically between 25 and  $200 \mu\text{mol L}^{-1}$ ; average oxygen concentrations were generally below  $100 \mu\text{mol L}^{-1}$ , and average chlorophyll-*a* concentrations were typically below  $60 \mu\text{g L}^{-1}$ .

Total dissolved inorganic nitrogen (TDIN = ammonium + nitrate + nitrite) consistently decreased from the early 1990s. In the 1996–2007 period, average TDIN concentrations decreased further from  $660 \mu\text{mol L}^{-1}$  to  $446 \mu\text{mol L}^{-1}$ . In the same period ammonium concentrations decreased from  $382 \mu\text{mol L}^{-1}$  to  $38 \mu\text{mol L}^{-1}$ , thus changing from being the most important fraction of TDIN to the least important. Also DIP concentrations decreased during this period, from on average  $26 \mu\text{mol L}^{-1}$  in 1996 to  $9.7 \mu\text{mol L}^{-1}$  in 2007. In the mid 1990s, average oxygen concentrations started to increase. In 1996, the average oxygen concentration was  $80 \mu\text{mol L}^{-1}$ , with on average only  $30 \mu\text{mol L}^{-1}$  during May–September. By 2007, the year round average had more than doubled to  $200 \mu\text{mol L}^{-1}$ , and the May–September average quintupled to  $170 \mu\text{mol L}^{-1}$ . In 2006 over-saturated oxygen levels were observed for the first time, caused by high primary production. In the same period, chlorophyll-*a* concentrations increased from on average  $18 \mu\text{g L}^{-1}$  to  $122 \mu\text{g L}^{-1}$ . Note that the higher average values in the 1980s and early 1990s are calculated from very few observations in these years (1–10 per year), making these data points less reliable. In 1969 and from 1996 onward, average values have been calculated from at least 50 observations each year.

An intriguing observation is the paradoxical decrease in nutrient concentrations and increase in oxygen concentrations, accompanied by increasing chlorophyll-*a* concentrations. This is contrary to the classical eutrophication response in estuarine and coastal systems, from which we would expect the highest annually averaged algal biomass to coincide with the highest annually averaged nutrient concentrations (Cloern, 2001; Smith, 2006). Light limitation was important but constant, given that SPM levels (governing light penetration in the estuary, Soetaert et al., 2006) remained similar (see also discussion). However, the environmental conditions in this hypereutrophied system, may have negatively affected algal growth. There is abundant evidence that extremely low oxygen concentrations negatively affect photosynthesis

**Table 1.** Data sources, number of data points (N) and average value for each year. Data sources: DP: DePauw (1975); W: Billen et al. (1985), Wollast (1988); A: Administration Zeeschelde; I: Belgian Institute for Hygiene and Epidemiology; V: Flemish Environmental Agency; C: Netherlands Institute of Ecology, NIOO-CEME; O: OMES project: Van Damme et al. (2005).

Oxygen [ $\mu\text{molL}^{-1}$ ]				Ammonium [ $\mu\text{molL}^{-1}$ ]			DIP [ $\mu\text{molL}^{-1}$ ]			chlorophyll- <i>a</i> [ $\mu\text{gL}^{-1}$ ]		
year	source	N	mean	source	N	mean	source	N	mean	source	N	mean
1967	DP	10	73	DP	2	377	DP	15	29			
1968	DP	20	69	DP	20	279	DP	46	23			
1969	DP	24	51	DP	24	490	DP	55	28	DP	50	11
1975	W	12	76	W	11	527	A	8	65			
1976	W	15	70	W	15	922	A	12	139			
1977	W, I	27	44	I, W	23	527	A, I	14	167			
1978	I, W	20	68	I, W	32	765	A, I	20	185			
1979	I	5	72	I	10	544	A, I	22	85			
1980	I	19	61	I	28	688	A, I	44	89			
1981	I	9	90	I	16	645	A, I	29	67			
1982	I, W	12	67	I, W	17	614	A, I	20	71	W	4	35
1983	I, W	10	77	I, W	15	336	A, I	23	64			
1984	I	4	79	I	8	900	A, I	16	30			
1985	I	4	48	I	8	449	A, I	17	44			
1986	I	4	66	I	8	777	A, I	17	142			
1987	I	4	43	I	8	491	I	8	158			
1988	I	5	136	I	10	424	I	10	209			
1989	I, V, C 21	81	I, C, V	35	571	I, C, V	19	107	C, V, I	7	55	
1990	I, V	19	74	V, I	30	582	I, V	31	66	I, V	6	45
1991	V, I	20	66	V, I	32	620	V, I, C	42	49	V, I	10	48
1992	V	15	79	V	24	596	C, V	39	47	V	1	56
1993	V	16	85	V	24	448	C, V	46	45	V	3	16
1995	O	7	108	V, O	31	459	C, V, O	40	20	O	6	4
1996	O	77	83	O	86	383	C, O, V	100	26	O	85	18
1997	O	77	78	O	59	389	O, C	80	25	O	70	67
1998	O	84	116	O	77	242	C, O	95	19	O	84	50
1999	O	70	86	O	75	214	C, O	87	18			
2000	O	89	141	O	90	192	C, O	95	17			
2001	O	84	164	O	84	107	O, C	95	11	O	84	59
2002	O	63	149	O	60	100	C, O	96	12	O	63	75
2003	O	67	142	O	67	100	O	67	13	O	67	117
2004	O	84	149	O	84	79	O	84	11	O	63	135
2005	O	77	160	O	77	110	O	84	19	O	77	109
2006	O	68	209	O	70	72	O	82	9	O	60	97
2007	O	77	199	O	77	37	O	83	10	O	71	123
2008	O	43	225	O	43	41	O	43	7	O	43	80

(Krause et al., 1985; Sundby and Schiött, 1992; Gong et al., 1993; Peckol and Rivers, 1995; Tyystjaervi, 2008) as well as metabolism (Kessler, 1974). Molecular sensors and regulatory genes related to low oxygen concentrations are present in most organisms (Wu, 2002). In such a reduced environment (Billen et al., 1988), benthic and pelagic sulfide production might have toxic effects on phytoplankton. And also elevated ammonium concentrations are known to be harmful to algae (Thomas et al., 1980; Bates et al., 1993; Kallqvist and Svenson, 2003). Therefore we hypothesize that algal growth was inhibited as a result of high organic waste and ammonia loading, leading to elevated ammonium concentrations, oxygen depletion and a strongly reduced environment.

### 3.2 A regime shift? A minimal mathematical model

One intuitively understands that the inhibition of algal growth may give rise to particular ecosystem behaviour. With high ammonium inputs (we focus on ammonium inputs, as nitrification is the major oxygen consuming process in the system under study), nitrification will cause a reduced, oxygen depleted environment and the introduced ammonium will not effectively get oxydized: algal growth will be inhibited although some algal biomass (and photosynthesis) will always be present due to upstream import. With low ammonia inputs, such a reduced, oxygen depleted environment will not exist and algal growth will not be inhibited. However, at certain intermediate ammonium input levels, the

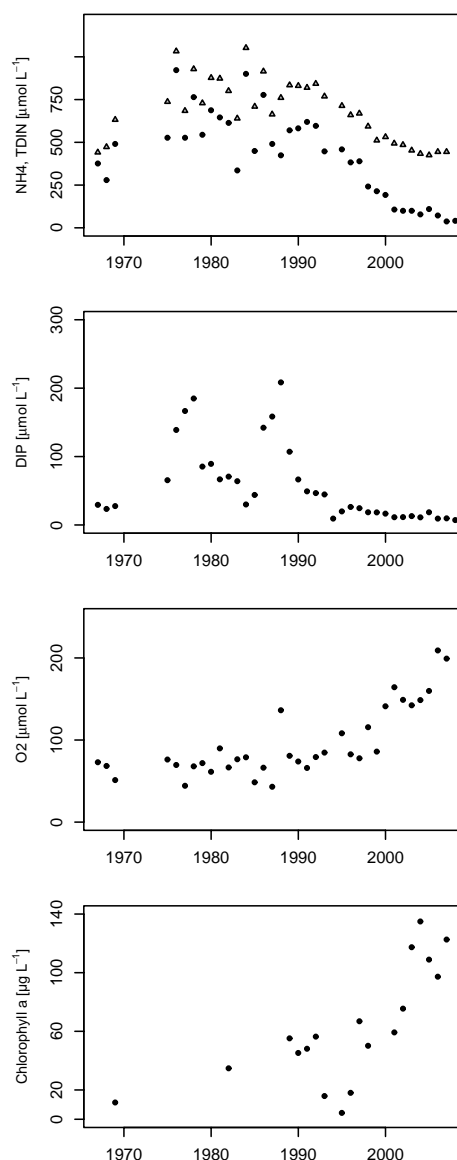


**Fig. 2.** Annual, FW averaged TDIN (triangles),  $\text{NH}_4$  (circles), DIP,  $\text{O}_2$  and chlorophyll-*a* concentrations from 1967 to 2007. Data compiled from different sources, with different sampling frequency. Only starting from 1996 the freshwater reach has been consistently monitored, with more than 50 measurements each year (see Table 1).

system might or might not evolve toward a hypoxic, algal growth inhibited situation (Fig. 3). Favorable weather conditions, higher influx of riverine phytoplankton or a higher oxygen concentration in the inflowing water will prevent the occurrence of algal growth inhibition, while other circumstances might cause the same ammonium load to lead to an algal growth inhibited situation.

We further explore the consequences of the inhibition of algal growth, by examining the steady states and transient behaviour of a simple mathematical model, designed to capture core features of ecosystem behaviour under over-enrichment

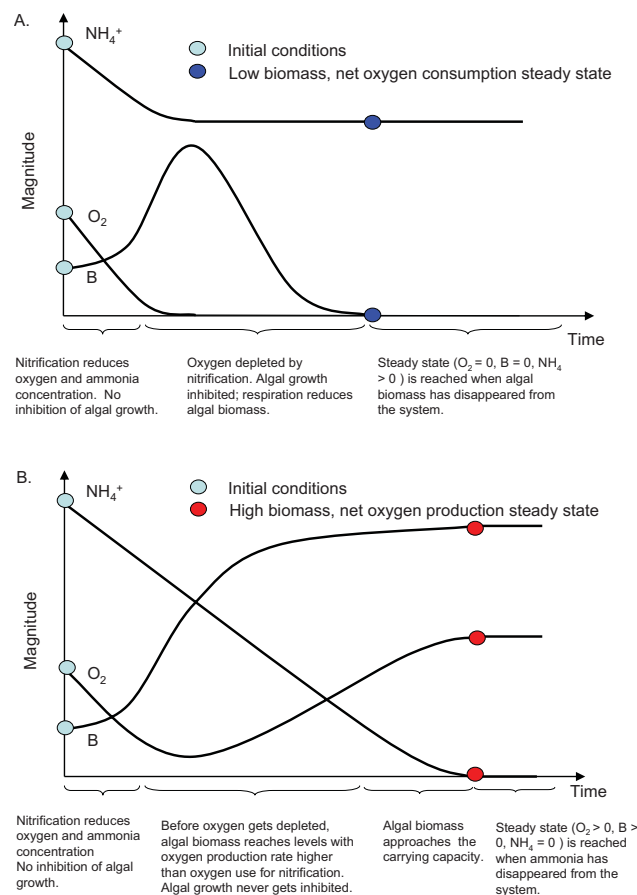


**Fig. 3.** Conceptual plot of transient evolution of the system state, with intermediate ammonia inputs. **(A)** Transient evolution of the system towards the low biomass, net oxygen consumption state. **(B)** With the same ammonium input rates, but slightly higher initial oxygen concentrations or algal biomass, with weather conditions favoring a slightly faster buildup of algal biomass, or with other fluctuations influencing the transient evolution of the system, anoxic conditions are never reached and the system evolves toward the high biomass, net oxygen production state.

with ammonium. The model consists of 3 state variables: algal biomass  $B$ , dissolved oxygen  $\text{O}_2$  and ammonium  $\text{NH}_4$ , and it can be considered as a one-box model of the whole freshwater reach. The following processes are taken into account: flushing ( $R_F$ ), net primary production (NPP), the difference between gross primary production (GPP) and autotrophic respiration ( $R_{\text{resp}}$ ), nitrification ( $R_{\text{nit}}$ ), and surface reaeration ( $R_{\text{aer}}$ ):

$$\frac{dB}{dt} = R_F(B) + F(\text{O}_2) \cdot \text{GPP} - R_{\text{resp}} \quad (1)$$

$$= R_F(B) + \text{NPP}$$

$$\frac{d\text{O}_2}{dt} = R_F(\text{O}_2) - \text{O:N} \cdot R_{\text{nit}} + \text{O:C} \cdot \text{NPP} + R_{\text{aer}} \quad (2)$$

$$\frac{d\text{NH}_4}{dt} = R_F(\text{NH}_4) - R_{\text{nit}} - \text{N:C} \cdot \text{NPP} \quad (3)$$

**Table 2.** Modelled processes. Process formulations are based on Soetaert and Herman (1995b), Regnier et al. (1997) and Hofmann et al. (2008).

Surface re-aeration	
$R_{\text{aer}}$	$= r_{\text{aer}} \cdot (\text{O}_2^{\text{sat}} - \text{O}_2)$
Nitrification	
$R_{\text{nit}}$	$= r_{\text{nit}} \cdot \frac{\text{O}_2}{\text{O}_2 + k_{\text{O}_2}} \cdot \frac{\text{NH}_4}{\text{NH}_4 + k_{\text{NH}_4}}$
Phytoplankton primary production, respiration and inhibition	
GPP	$= \mu_{\text{max}} \cdot \left(1 - \frac{B}{K}\right) \cdot B$
$R_{\text{resp}}$	$= R_m \cdot B$
$F(\text{O}_2)$	$= \frac{\text{O}_2}{\text{O}_2 + k_{\text{O}_2}}$
Flushing	
$R_F([\cdot])$	$= \frac{Q}{V} ([\cdot])^{up} - [\cdot])$ with $[\cdot] = B, \text{O}_2$ or $\text{NH}_4$

Standard formulations for all processes are used (Table 2) with parameter values that are realistic for the freshwater Schelde, based on Soetaert and Herman (1995b), Regnier et al. (1997) and Hofmann et al. (2008) (Table 3). A carrying capacity  $K$  is included to impose an upper limit on algal biomass, e.g. due to self-shading. We assume that nutrients never limit algal growth, and in particular we assume that algae switch to nitrate as a nitrogen source at low ammonium concentrations. This assumption makes sense since TDIN and DIP levels were always higher than  $60 \mu\text{mol L}^{-1}$  and  $4 \mu\text{mol L}^{-1}$  respectively. The feature of interest, however, is the inclusion of a factor  $F(\text{O}_2)$  that represents the adverse effect of low oxygen concentrations on photosynthesis (we leave out potential ammonium toxicity from the current analysis, and we assume that this formulation also accounts for effects of the production of harmful substances in a reduced environment). We construct  $F(\text{O}_2)$  as a Monod function of oxygen concentration, with a half saturation concentration of  $1 \mu\text{mol L}^{-1}$ . Essentially, incorporation of this factor reduces primary production continuously at decreasing low oxygen concentrations; when oxygen concentrations decrease from  $10$  to  $0 \mu\text{mol L}^{-1}$ , calculated primary production is reduced from 90% of maximal production to 0.

The steady states of this model depend on the upstream ammonium concentration (Fig. 4, central panel). With high upstream ammonium, the steady state ammonium concentration is higher than zero, nitrification forces oxygen to low values and primary production is inhibited. In this steady state, the calculated ratio of algal oxygen production to the sum of autotrophic respiration and oxygen consumption by nitrifiers ( $P/R = F(\text{O}_2) \cdot \text{GPP} / (R_{\text{resp}} + \text{O:N} \cdot R_{\text{nit}})$ ) is lower than 1, and we refer to it as the low biomass, net oxygen consumption state. Conversely, at low upstream ammonium concentration the steady state is characterized by high oxy-

**Table 3.** Process and stoichiometric parameters, and upstream boundary conditions. Parameters values are taken from Soetaert and Herman (1995b); Regnier et al. (1997) and Hofmann et al. (2008).

Surface re-aeration		
$r_{\text{aer}}$	$= 0.05$	$\text{d}^{-1}$
$\text{O}_2^{\text{sat}}$	$= 300$	$\text{mmol m}^{-3}$
Nitrification		
$r_{\text{nit}}$	$= 70$	$\text{mmol m}^{-3} \cdot \text{d}^{-1}$
$k_{\text{O}_2}$	$= 1$	$\text{mmol m}^{-3}$
$k_{\text{NH}_4}$	$= 5$	$\text{mmol m}^{-3}$
O:N	$= 1.89$	$\text{mmol O}_2 (\text{mmol NH}_4)^{-1}$
Phytoplankton primary production, respiration and inhibition		
$\mu_{\text{max}}$	$= 1$	$\text{d}^{-1}$
$K$	$= 700$	$\text{mmol C m}^{-3}$ (fitted)
$R_m$	$= 0.25$	$\text{d}^{-1}$
O:C	$= 1$	$\text{mmol O}_2 (\text{mmol C})^{-1}$
N:C	$= 0.15$	$\text{mmol N} (\text{mmol C})^{-1}$
Chl:C	$= 15$	$\text{mg C} (\text{mg Chl})^{-1}$
$k_{\text{O}_2}$	$= 1$	$\text{mmol m}^{-3}$
Flushing		
$\frac{Q}{V}$	$= 0.14$	$\text{d}^{-1}$
Upstream boundary conditions		
$B^{up}$	$= 50$	$\text{mmol C m}^{-3}$
$\text{O}_2^{up}$	$= 100$	$\text{mmol O}_2 \text{ m}^{-3}$

gen concentrations and algal biomass, and low ammonium concentrations. In this case the  $P/R$ -ratio is higher than 1, and we refer to this state as the high biomass, net oxygen production state (Fig. 5).

At intermediate upstream ammonium concentrations, however, the system displays both a low biomass, net oxygen consumption and a high biomass, net oxygen production state, and between the two stable states, an unstable equilibrium is found (Fig. 5). Depending on the initial conditions, the system will evolve to either of the steady states. It follows also that with decreasing upstream ammonium concentration and equal initial conditions, the system will abruptly change from a low biomass, net oxygen consumption to a high biomass, net oxygen production steady state when the upstream ammonium concentration drops below a critical threshold. As such, the model features a *regime shift* triggered by a change in ammonium input.

To link model output to observations, we first note that the steady state calculations do not account for seasonal and spatial patterns. We might, however, reasonably expect that the most downstream observed concentrations in the FW reach, will most closely reflect the steady state conditions. As there

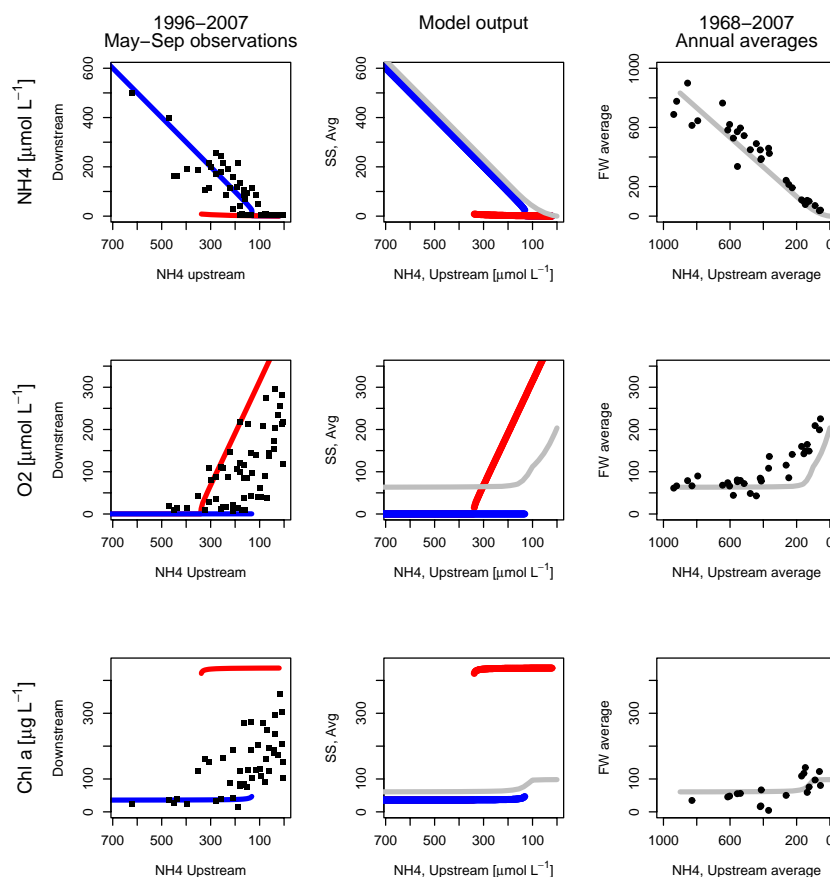


**Fig. 4.** Steady state and averaged model output (central panel). The model displays a *low biomass, net oxygen consumption state* (high ammonium, low oxygen and low chlorophyll-*a* concentrations; blue line) at high upstream ammonium concentration and an *high biomass, net oxygen production state* (low ammonium, high oxygen and high chlorophyll-*a* concentrations; red line). Steady state output is compared with data from the downstream station plotted against ammonium concentrations at the upstream station for the years 1996–2007 (left panel). The calculated proxy for the annual, FW average (grey line) is compared with annual, FW averaged data from 1968–2007 plotted against annual averaged upstream ammonia concentration (right panel). See text for detailed information.

is only significant phytoplankton growth from late spring to early autumn, we compare all May–September observations from this downstream station (plotted against total ammonium concentrations of the upstream monitoring station) with steady state model output (Fig. 4, left panel). Despite the highly simplified nature of the model, its numerical output is remarkably realistic, and its steady state characteristics seem consistent with the data (we note that no fine-tuning or calibration of parameters was performed, except for the carrying capacity ( $K$ ) of algal biomass, visually fitted to embrace all chlorophyll-*a* observations between the high and low steady state of modelled chlorophyll-*a*). With upstream ammonium concentration below  $100 \mu\text{mol L}^{-1}$ , observed ammonium concentration at the downstream station are always zero, and observed oxygen and chlorophyll-*a* concentrations are distinctly different from zero. At upstream ammonium concentrations above  $350 \mu\text{mol L}^{-1}$ , only high ammonium, low oxygen and low chlorophyll-*a* are observed. At intermediate upstream ammonium concentrations

(between  $100$  and  $350 \mu\text{mol L}^{-1}$ ) a mixture of both situations can be observed, with a finite subset of data points reflecting the low biomass, net oxygen consumption state, with high ammonium, low oxygen and low chlorophyll-*a* concentrations.

The calculated high biomass, net oxygen production steady state provides an upper limit for oxygen and chlorophyll-*a* concentration, rather than being distinguishable as an alternate state in the observations. This is not surprising, since the calculations were performed with fixed upstream boundary conditions, algal productivity and flushing rate, while in reality these quantities are not constant between May and September (Fig. 4). The model parameterization seems to be satisfactory for conditions favoring maximal production (low discharge, high light). Moreover, a system in which the oxygen concentrations are governed mainly by the net effect of nitrification and primary production, can be expected to have short term fluctuations in oxygen concentration, responding to fluctuations in discharges, incident



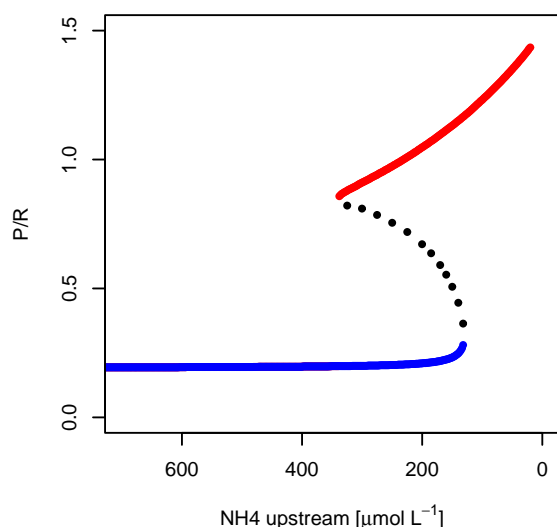


**Fig. 5.** The ratio of oxygen production (algae) and consumption (respiration and nitrification) at steady state (full lines) and at the unstable equilibria of the system (dotted line).

light, boundary conditions, etc. In particular, peak discharges (which cause a partial flushing out of algal biomass) and cloudy weather conditions (with lower incident light) may reduce the oxygen production below the demand for nitrification and may induce (sharp) decreases in observed oxygen concentrations.

Although the monthly sampling is probably not frequent enough to observe these (short term) fluctuations, it can be considered as random sampling of these fluctuating oxygen concentrations, and should therefore also display fluctuations. Figure 5 shows the annual pattern of oxygen concentrations at the downstream station for the 1996–2007 period. During 1996–2002, oxygen concentrations show a clear seasonal pattern, with high oxygen concentrations in winter, and low concentrations in summer and autumn. Starting from 2003, this pattern becomes more irregular, and in particular 2004–2006 oxygen concentration show large fluctuations during summer months, with maximal differences between high and low concentrations of more than  $200 \mu\text{mol L}^{-1}$ .

Additional model calculations were performed to produce output comparable to the annual, FW averaged values (Fig. 2). To account for seasonal variability, we calculated model output at temperatures 5–20°C (step size 1°C) with the model extended with a classic Q10-formulation for temperature dependence of biological process rates. Since discharges and upstream oxygen concentrations are typically larger in winter, we performed the simulations at different temperatures with flushing rates and upstream oxygen concentrations based on a linear regression against temperature from the 1996–2007 dataset. Finally we calculated the 15-day average of transient model output starting from the initial conditions set equal to upstream boundary concentrations, as a proxy for the FW ecosystem average, under the

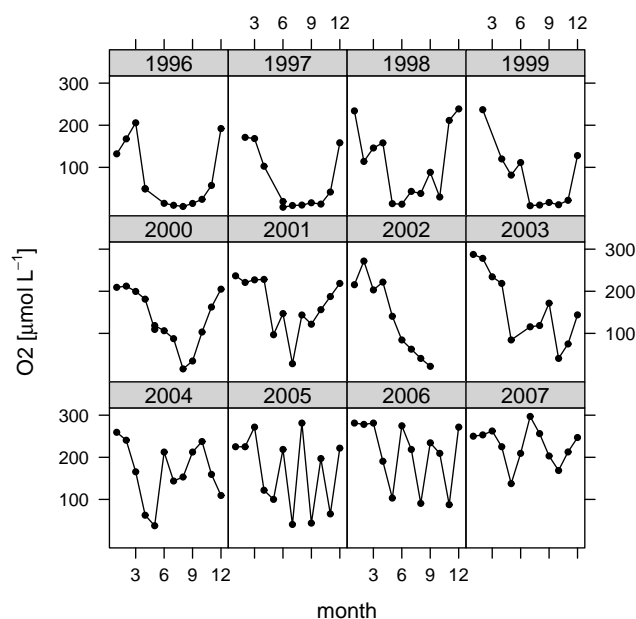


**Fig. 6.** Annual pattern of dissolved oxygen at the downstream station.

assumption that the real ecosystem evolves towards steady state along the estuarine axis. The resulting proxy for annual, FW averaged values shows a continuous, although non-linear response to decreasing ammonium inputs (Fig. 4, central panel). Again this simple approximation gives realistic numerical output when compared to observed data. The right panel of Fig. 4 shows observed annual, FW averaged ammonium, oxygen and chlorophyll-*a* concentrations plotted against observed annual averaged upstream ammonium concentrations, for the available data between 1968 and 2007. We note that no fine-tuning or calibration of parameter values was performed, except for the choice of the integration interval of 15 days, which resulted in a visually better proxy for the observed average values than other trial intervals of 7, 10 and 20 days.

#### 4 Discussion

Based on a long term data set of dissolved oxygen, total ammonium, dissolved inorganic phosphorus and chlorophyll-*a*, we demonstrated that the freshwater Schelde estuary has changed over a relatively short period of time from a system with persistent hypoxia, elevated ammonium concentrations and limited algal biomass, to a system with low ammonium concentrations, where hypoxia is virtually nonexistent and in which autotrophic production has become increasingly important. The paradoxical increase in algal biomass with decreasing nutrient inputs was contrary to expectations from the classical eutrophication response of estuarine and coastal systems. This stimulated us to investigate the potential



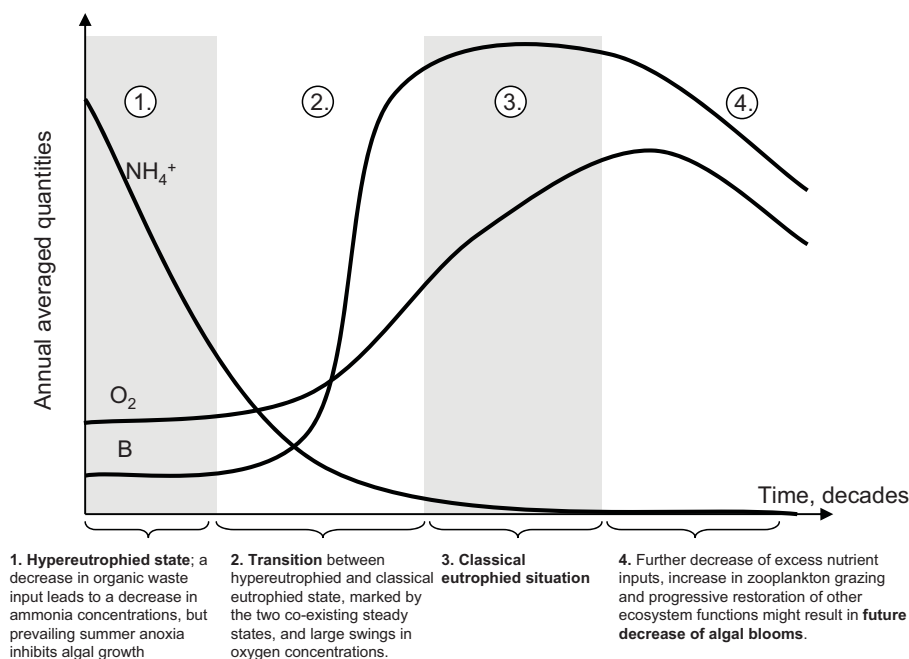


**Fig. 7.** Conceptual scheme describing the recovery from hypereutrophication. The evolution of the freshwater Schelde from stage 1 to stage 3 is described in this manuscript. Most eutrophication reversal studies deal with stage 4.

causes of low algal biomass observed until the late 1990s. We concluded that it is plausible that high ammonium concentrations, persistent hypoxia or the production of harmful substances in such a reduced environment, inhibited algal growth and photosynthesis during most of the time span of our data set.

To our knowledge, such elevated ammonium concentrations and such prolonged periods of severe hypoxia, as observed in the (freshwater) Schelde, have not been recorded in any of the major documented riverine or estuarine ecosystems. Published data sets on other systems that could have been similarly degraded, might be lacking relevant periods or areas. As such the freshwater Schelde provides a unique and fairly well documented instance of hypereutrophic systems. Most other studies on eutrophication reversal document recovery starting from the point where the freshwater Schelde is today. This is illustrated in Fig. 7, in which we discern four main stages in the recovery from hypereutrophication. Stage 1 is the hypereutrophied state, characterized by extreme high ammonia inputs and associated hypoxia/anoxia and algal growth inhibition. Stage 2, a transitional stage, represents the recovery from this hypereutrophied state towards the classical eutrophied state. According to our study, this stage is marked by two co-existing steady states and large swings in oxygen concentrations. The third stage represents the classical, often studied eutrophied state, with intense algal blooms due to excess inorganic nutrient availability. The final stage refers to the recovery of aquatic systems from eutrophication. Our study describes biogeochemical mech-

anisms and dynamics in the first two stages. Almost all studies on eutrophication, trend reversal and biomanipulation, deal with stages 3 and 4. In many regions in the world however, organic matter and nutrient load to aquatic systems are still increasing (Diaz and Rosenberg, 2008). In the upper reaches of the Chinese Pearl river for example, similar ammonium and oxygen concentrations have recently been measured (Harrison et al., 2008). Unfortunately no information about primary production or algal biomass in this system is available.

We have deliberately chosen a simple mathematical model to explore and highlight the core features of a system governed by the described mechanisms. This makes direct comparison of model output to observed data more difficult. In particular, constant upstream boundary conditions, algal productivity and flushing rate, are important simplifications. Also the averaging procedure, as a proxy for annual, FW averaged values, is only an approximation to illustrate that averaged output of a model that clearly displays a regime shift, can show a continuous response. A more complex multi-dimensional model, incorporating more processes and real forcing functions and boundary conditions, might reproduce spatio-temporal patterns, but this is outside the scope of this article and would not change the essential findings. In particular, the inclusion of allochthonous organic matter degradation would not change the qualitative behavior of the model nor make it more close to a realistic ecosystem model. The additional oxygen consumption associated with this process is implicitly taken into account by our model parameterization,

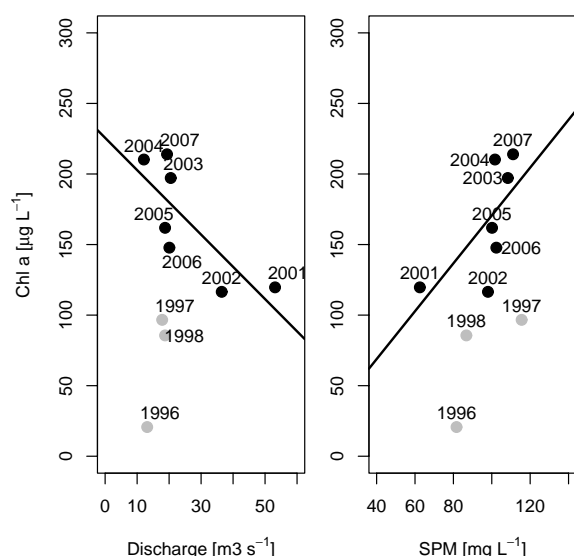


**Fig. 8.** May–September and FW averaged chlorophyll-*a* concentrations versus average discharge ( $Q$ ) and average suspended matter concentration (SPM), with linear regression lines for data points after 1999. There exists no correlation for the whole 1996–2007 data set (black and grey symbols). For the 2001–2007 data set (black symbols), average chlorophyll-*a* concentration is negatively correlated with average discharge ( $r^2=0.62$ ,  $p=0.04$ ), and weakly positively correlated with suspended matter concentration ( $r^2=0.44$ ,  $p=0.1$ ).

and organic matter input is decreasing along with ammonia inputs. Of course this simplification becomes invalid when ammonia concentrations cease to be a proxy for organic matter availability. This will for instance be the case for future stages of the recovery (stages 3 and 4, Fig. 7). Also other simplifications might become invalid, e.g. the omission of benthic processes, higher trophic levels and nutrient limitations. While the presented model has high explanatory value for the system dynamics to date, this will not necessarily be the case for future evolutions.

The correspondence of the output of this very simple model with observed data, without any parameter fine-tuning, represents a strong argument in favor of the proposed hypothesis of algal growth inhibition, and a posteriori justifies the focus on the limited number of processes. Furthermore, the “classical” regime shift literature either focuses on conceptual, theoretical, dimensionless models (e.g. Duarte et al., 2009; Kemp et al., 2009), applies statistical tools to test observed data on the existence of jumps as an indication for regime shifts, or develops indicators to predict potential future shifts or collapses (e.g. Scheffer and Carpenter, 2003; Carpenter et al., 2008). Although simple, our model is realistic and produces interpretable, quantitative output that can be linked with observed data. The parameterization of the proposed mechanisms that produces the shift, is realistic, and the theoretical jumps have amplitudes that correspond with observations.

The model results indicate that, with the mechanisms described, the recovery of hypereutrophic systems can display a threshold-like and non-linear behaviour. Whether or not the recovery can be termed a regime shift partly depends on the chosen definition. Some authors use a more loose and pragmatic definition (e.g. deYoung et al., 2008), while others use a more strict definition that strictly separates steep gradual responses from actual jumps between alternative stable states (e.g. Schroder et al., 2005). Much of the evidence for multiple steady states is drawn from mathematical or numerical model results, and it is a long standing debate whether or not multiple steady states do exist in nature, and if so whether it is possible to demonstrate their existence based on field data (Connell and Sousa, 1983; Scheffer and Carpenter, 2003). The observed change in the freshwater Schelde to increasing autotrophy over a few years, after decades of persistent hypoxia and hypereutrophication, could certainly be termed a regime shift in the loose sense. The presented mathematical model also features a regime shift in the strict sense.

To our knowledge this is the first account of mathematically well defined multiple stable states in a flow-through system. Research on non-linear dynamics has focused on enclosed systems in which the dynamics is governed primarily by internal processes and less by physical forcing. In such systems, the manifestations of multiple steady states are more obvious, whereas in flow-through systems that are strongly influenced by external forcings, shifts may be masked by (predictable) variability. In our case, the model of the freshwater Schelde displays a low biomass, net oxygen consumption stable state and a high biomass, net oxygen production stable state, co-existing at intermediate levels of ammonia load. This is most comprehensibly summarized in Fig. 5 showing the ratio of oxygen production over the oxygen consumption by nitrifiers and autotrophic respiration ( $P/R$ ). However, seasonality of the drivers of the system partly masks these ecosystem properties, as shown in the comparison with observed data in Fig. 4. Only with incident light levels ensuring maximal phytoplankton production and with sufficiently low discharges to prevent flushing out of algal biomass,  $P/R > 1$  will be observed in the real system. As demonstrated in Fig. 4, the chosen model parameterization results in the calculation of upper and lower limits of observables.

At first sight, a direct adverse effect of extreme hypoxia on algal growth might seem contradictory, since algae themselves produce oxygen through photosynthesis. However, the Schelde is well mixed and light penetration is very limited (Kromkamp and Peene, 1995; Soetaert et al., 2006). Consequently algal cells frequently reside in deeper, dark water masses. Thus, not only during the night, these algal cells are exposed to respiratory and diffusive oxygen loss to the surrounding hypoxic water, which they can not compensate by photosynthetic production. Also when they are exposed to low to moderate light intensities, photosynthetic production might not be sufficient to compensate the oxygen loss

due to the steep inner to outer cell oxygen gradient and algal respiration taken together. As such, when extracellular oxygen concentrations are sufficiently low, algal cells will have to resort to less efficient anaerobic metabolism (Kessler, 1974), during a considerable fraction of time. A similar argumentation holds for increased sensitivity to photoinhibition under extreme hypoxia. Algal cells traveling from upper to deeper water layers might first be confronted with high light intensities inducing photoinhibition, and next be transported to dark, hypoxic water layers in which they can not recover from photoinhibitory effects (Sundby and Schiött, 1992; Tyystjaervi, 2008). Finally, a molecular oxygen sensor is probably present in all cells, and regulatory genes related to low oxygen concentrations, downregulating protein synthesis and suppressing cell growth during hypoxia to save energy for essential metabolic processes, might also be present in phytoplankton (Wu, 2002).

We have not included potential ammonium toxicity in the model calculations. A system with a well chosen ammonium toxicity function (with a steep enough response curve) would also display two alternative stable states without any inhibition by hypoxia. But to explain the low biomass state at upstream ammonium concentrations equal to or higher than  $200 \mu\text{mol L}^{-1}$ , we would have to assume an ammonium toxicity threshold of about  $100 \mu\text{mol L}^{-1}$ , as this is the steady state ammonium concentration corresponding with this upstream ammonium concentration (Fig. 4). This is at the lower end of reported ammonium concentrations with inhibitory effects on algal growth, and insensitivity to much higher concentrations (up to  $440 \mu\text{mol L}^{-1}$ ) of marine algal species have also been found (Thomas et al., 1980; Bates et al., 1993; Kallqvist and Svenson, 2003). Nevertheless, a combined effect of hypoxia and ammonium inhibition remains a possibility and, since they are correlated, could reinforce each other. In general the mechanisms for inhibition of photosynthesis or algal growth by elevated ammonium concentrations and severe hypoxia are rather poorly understood. Laboratory experiments to investigate the (combined) effects of stressors on the currently flourishing phytoplankton communities, can provide more insight, but they are currently lacking.

In freshwater systems, regime shifts related to eutrophication and oligotrophication are usually studied based on dissolved inorganic phosphorus concentrations, as most freshwater bodies are P-limited (Dent et al., 2002). Although the river Schelde also showed very large changes in DIP (Fig. 4), it should be realized that ammonium is not only a nutrient like phosphorus, but also a substrate for nitrifiers, and thus directly influence oxygen consumption. In contrast, dissolved inorganic phosphorus concentrations principally depend on oxygen via redox-controlled Fe-P interactions.

While the presented data give indication for an adverse effect of hypereutrophication as described above, we cannot exclude other factors, such as climatic variability, playing a role in this apparent shift from the low algal biomass, net oxygen consumption state to high algal biomass, net

oxygen production state. However no relationship between summer averaged chlorophyll-*a* concentrations, and flushing discharge and suspended matter concentration respectively, was observed for the 1996–2007 data set (Fig. 7). This indicates that the two main drivers typically invoked to justify changes in riverine and estuarine primary production, flushing rate (discharge) and light conditions (e.g. Howarth et al., 2000), are not correlated with the observed increase in average chlorophyll-*a* concentrations. When considering only the data after 2000, average summer chlorophyll-*a* concentrations are negatively correlated with average summer discharge ( $r^2 = 0.62$ ,  $p = 0.04$ ), and weakly positively correlated with average suspended matter concentration ( $r^2 = 0.44$ ,  $p = 0.1$ ) (Fig. 7). The latter suggests that increased algal blooms is reflected in the observed suspended matter concentrations. The negative correlation with discharge for the data from 2001–2007 suggests that whereas long-term changes in chlorophyll-*a* concentrations can not be explained by the common drivers, inter-annual variability in the current state is primarily determined by physical forcing, consistent with model simulations of Arndt et al. (2007).

Zooplankton grazing, another common controlling factor of phytoplankton biomass, likely has increased over the last decade, in accordance with the observed increasing zooplankton abundance (Tackx et al., 2005). Thus, *ceteris paribus*, we would expect a decrease rather than an increase in phytoplankton biomass. In addition, toxic pollutants are surprisingly poorly documented for the Schelde estuary. A recent study on chlorotriazines, found maximum atrazine concentrations of  $736 \text{ ng L}^{-1}$  at the downstream boundary of the freshwater Schelde (Noppe et al., 2007). This is one order of magnitude lower than concentrations with inhibitory effect on algal growth (Tang et al., 1997).

European estuaries, including the Schelde, have been characterized as strongly heterotrophic ecosystems (Heip et al., 1995; Gazeau et al., 2005; Soetaert et al., 2006). The balance between heterotrophic, photo-autotrophic and chemo-autotrophic production in the freshwater Schelde has changed significantly over the last decade. Our results suggest that photo-autotrophic processes have become increasingly important both in the carbon and oxygen balances. At least periodically the system is autotrophic and net oxygen producing. The net annual metabolic status is more difficult to assess, as it heavily depends on the strongly peaking phytoplankton biomass and the seasonal variability in reaction rates of nitrification and heterotrophic activity.

With further decreasing ammonium inputs and increasing oxygen concentration, the system may develop toward a more natural foodweb and mode of ecosystem functioning, as indicated by the repopulation of the brackish and freshwater reaches by zooplankton (Appeltans et al., 2003; Tackx et al., 2005). In the future, zooplankton grazing might become a significant factor controlling phytoplankton biomass. As suggested by Strayer et al. (2008), the evolution toward a condition in which phytoplankton biomass is

(partly) controlled by zooplankton grazing might also proceed rapidly, possibly inducing the next 'step' in the recovery of the freshwater Schelde. In such a system also higher trophic levels, including zooplanktivorous and piscivorous fish may gain in importance, causing further changes in trophic structure and the balance between biological and physical control.

**Acknowledgements.** This research received partial funding from the Flemish project OMES, funded by W&Z NV, the Netherlands Organisation of Scientific Research (PIONIER) and the EU (HYPOX). Eric Struyf and Daniel Conley acknowledge EU Marie Curie Actions (SWAMP MEIF-CT-2006-040534, COMPACT MEXC-CT-2006-042718) for funding. Eric Struyf acknowledges FWO (Flemish Research Foundation) for his postdoc grant. This is publication 4683 of the Netherlands Institute of Ecology (NIOO-KNAW).

Edited by: T. J. Battin

## References

- Appeltans, W., Hannouti, A., Van Damme, S., Soetaert, K., Vanthomme, R., Tackx, M., and Meire, P.: Zooplankton in the Schelde estuary (Belgium/The Netherlands). The distribution of *Eurytemora affinis*: Effect of oxygen?, *J. Plankton Res.*, 25, 1441–1445, 2003.
- Arndt, S., Vanderborgh, J. P., and Regnier, P.: Diatom growth response to physical forcing in a macrotidal estuary: Coupling hydrodynamics, sediment transport, and biogeochemistry, *J. Geophys. Res.*, 112, C05045, doi:10.1029/2006JC003581, 2007.
- Bates, S. S., Worms, J., and Smith, J. C.: Effects Of Ammonium And Nitrate On Growth And Domoic Acid Production By *Nitzschia-Pungens* In Batch Culture, *Can. J. Fish. Aquat. Sci.*, 50, 1248–1254, 1993.
- Billen, G.: Nitrification In Scheldt Estuary – (Belgium And Netherlands), *Estuar. Coast. Mar. Sci.*, 3, 79–89, 1975.
- Billen, G., Somville, M., Debecker, E., and Servais, P.: A Nitrogen Budget Of The Scheldt Hydrographical Basin, *Neth. J. Sea. Res.*, 19, 223–230, 1985.
- Billen, G., Lancelot, C., De Becker, E., and Servais, P.: Modelling microbial processes (phyto- and bacterioplankton) in the Schelde estuary, *Hydrobiological Bulletin*, 22 pp., 1988.
- Billen, G., Garnier, J., and Rousseau, V.: Nutrient fluxes and water quality in the drainage network of the Scheldt basin over the last 50 years, *Hydrobiologia*, 540, 47–67, ECSA Scheldt Estuary, 2005.
- Carpenter, S., Caraco, N., Correll, D., Howarth, R., Sharpley, A., and Smith, V.: Nonpoint pollution of surface waters with phosphorus and nitrogen, *Ecol. Appl.*, 8, 559–568, 1998.
- Carpenter, S., Ludwig, D., and Brock, W.: Management of eutrophication for lakes subject to potentially irreversible change, *Ecol. Appl.*, 9, 751–771, 1999.
- Carpenter, S. R., Brock, W. A., Cole, J. J., Kitchell, J. F., and Pace, M. L.: Leading indicators of trophic cascades, *Ecol. Lett.*, 11, 128–138, 2008.
- Cloern, J. E.: Our evolving conceptual model of the coastal eutrophication problem, *Mar. Ecol.-Prog. Ser.*, 210, 223–253, 2001.
- Conley, D. J., Carstensen, J., Vaquer-Sunyer, R., and Duarte, C. M.: Ecosystem thresholds with hypoxia, *Hydrobiologia*, 629(1), 21–29, doi:10.1007/s10750-009-9764-2, 2009.
- Connell, J. and Sousa, W.: On the evidence needed to judge ecological stability or persistence, *Am. Nat.*, 121, 789–824, 1983.
- de Bie, M., Starink, M., Boschker, H., Peene, J., and Laanbroek, H.: Nitrification in the Schelde estuary: methodological aspects and factors influencing its activity, *FEMS Microbiol. Ecol.*, 42, 99–107, 2002.
- de Jong, D. and De Jonge, V.: Dynamics and distribution of microphytobenthic chlorophyll-a in the Western Scheldt estuary (SW Netherlands), *Hydrobiologia*, 311, 21–30, 1995.
- De Pauw, C.: Bijdrage tot de kennis van milieu en plankton in het Westerschelde-estuarium, Contribution to the knowledge of the environment and plankton in the Westerschelde-estuary, Ph.D. thesis, University of Gent, 1975 (in Dutch).
- Dent, C., Cumming, G., and Carpenter, S.: Multiple states in river and lake ecosystems, *Philos. T. Roy. Soc. B*, 357, 635–645, 2002.
- deYoung, B., Barange, M., Beaugrand, G., Harris, R., Perry, R. I., Scheffer, M., and Werner, F.: Regime shifts in marine ecosystems: detection, prediction and management, *Trends Ecol. Evol.*, 23, 402–409, 2008.
- Diaz, R. J. and Rosenberg, R.: Spreading dead zones and consequences for marine ecosystems, *Science*, 321, 926–929, 2008.
- Duarte, C. M., Conley, D. J., Carstensen, J., and Sánchez-Camacho, M.: Return to Neverland: Shifting Baselines Affect Eutrophication Restoration Targets, *Estuar. Coast.*, 32(1), 29–36, 2009.
- Elliott, M. and McLusky, D. S.: The need for definitions in understanding estuaries, *Estuar. Coast. Shelf Sci.*, 55, 815–827, 2002.
- Frankignoulle, M., Abril, G., Borges, A., Bourge, I., Canon, C., DeLille, B., Libert, E., and Theate, J. M.: Carbon dioxide emission from European estuaries, *Science*, 282, 434–436, 1998.
- Garnier, J. and Billen, G.: Production vs. Respiration in river systems: An indicator of an "ecological status", *Sci. Total. Environ.*, 375, 110–124, 2007.
- Gazeau, F., Gattuso, J. P., Middelburg, J. J., Brion, N., Schiettecatte, L. S., Frankignoulle, M., and Borges, A. V.: Planktonic and whole system metabolism in a nutrient-rich estuary (the Scheldt estuary), *Estuaries*, 28, 868–883, 2005.
- Gong, H., Nilsen, S., and Allen, J.: Photoinhibition of photosynthesis *in vivo* – involvement of multiple sites in a photodamage process under CO<sub>2</sub>-free and O<sub>2</sub>-free conditions, *Biochim. Biophys. Acta*, 1142, 115–122, 1993.
- Gypens, N., Borges, A. V., and Lancelot, C.: Effect of eutrophication on air-sea CO<sub>2</sub> fluxes in the coastal Southern North Sea: a model study of the past 50 years, *Glob. Change Biol.*, 15, 1040–1056, 2009.
- Harrison, P. J., Yin, K., Lee, J. H. W., Gan, J., and Liu, H.: Physical-biological coupling in the Pearl River Estuary, *Cont. Shelf Res.*, 28, 1405–1415, 2008.
- Heip, C. H. R., Goosen, N. K., Herman, P. M. J., Kromkamp, J., Middelburg, J. J., and Soetaert, K.: Production and consumption of biological particles in temperate tidal estuaries, *Oceanogr. Mar. Biol.*, 33, 1–149, 1995.
- Hofmann, A. F., Soetaert, K., and Middelburg, J. J.: Present nitrogen and carbon dynamics in the Scheldt estuary using a novel 1-D model, *Biogeosciences*, 5, 981–1006, 2008, <http://www.biogeosciences.net/5/981/2008/>.
- Howarth, R., Swaney, D., Butler, T., and Marino, R.: Climatic con-

- trol on eutrophication of the Hudson River estuary, *Ecosystems*, 3, 210–215, 2000.
- Kallqvist, T. and Svenson, A.: Assessment of ammonia toxicity in tests with the microalga, *Nephroselmis pyriformis*, Chlorophyta, *Water. Res.*, 37, 477–484, 2003.
- Kemp, W. M., Testa, J. M., Conley, D. J., Gilbert, D., and Hagy, J. D.: Coastal hypoxia responses to remediation, *Biogeosciences Discuss.*, 6, 6889–6948, 2009, <http://www.biogeosciences-discuss.net/6/6889/2009/>.
- Kessler, E.: Hydrogenase, photoreduction and anaerobic growth, in: *Algal physiology and biochemistry*, edited by: Steward, W., Blackwell scientific publications, Oxford, 456–473, 1974.
- Krause, G., Koster, S., and Wong, S.: Photoinhibition of photosynthesis under anaerobic conditions studied with leaves and chloroplasts of *spinacia-oleracea* L., *Planta*, 165, 430–438, 1985.
- Kromkamp, J. and Peene, J.: On the possibility of net primary production in the turbid Schelde estuary (SW Netherlands), *Mar. Ecol.-Prog. Ser.*, 121, 249–259, 1995.
- Kromkamp, J., Peene, J., Vanrijswijk, P., Sandee, A., and Goosen, N.: Nutrients, Light And Primary Production By Phytoplankton And Microphytobenthos In The Eutrophic, Turbid Westerschelde Estuary (The Netherlands), *Hydrobiologia*, 311, 9–19, 1995.
- Lancelot, C., Gypens, N., Billen, G., Garnier, J., and Roubeix, V.: Testing an integrated river-ocean mathematical tool for linking marine eutrophication to land use: The *Phaeocystis*-dominated Belgian coastal zone (Southern North Sea) over the past 50 years, *J. Marine Syst.*, 64, 216–228, 2007.
- Lancelot, C., Spitz, Y., Gypens, N., Ruddick, K., Becquevort, S., Rousseau, V., Lacroix, G., and Billen, G.: Modelling diatom and *Phaeocystis* blooms and nutrient cycles in the Southern Bight of the North Sea: the MIRO model, *Mar. Ecol.-Prog. Ser.*, 289, 63–78, 2005.
- Meire, P., Ysebaert, T., Van Damme, S., Van den Bergh, E., Maris, T., and Struyf, E.: The Scheldt estuary: a description of a changing ecosystem, *Hydrobiologia*, 540, 1–11, 2005.
- Noppe, H., Ghekiere, A., Verslycke, T., De Wulf, E., Verheyden, K., Monteyne, E., Polfliet, K., van Caeter, P., Janssen, C. R., and De Brabander, H. F.: Distribution and ecotoxicity of chlorotriazines in the Scheldt Estuary (B-NI), *Environ. Pollut.*, 147, 668–676, 2007.
- Oguz, T. and Gilbert, D.: Abrupt transitions of the top-down controlled Black Sea pelagic ecosystem during 1960–2000: Evidence for regime-shifts under strong fishery exploitation and nutrient enrichment modulated by climate-induced variations, *Deep-Sea Res. I*, 54, 220–242, 2007.
- Owens, N.: Estuarine nitrification: a naturally occurring fluidized bed reaction?, *Estuar. Coast. Shelf. Sci.*, 22, 31–44, 1986.
- Peckol, P. and Rivers, J. S.: Physiological responses of the opportunistic macroalgae *Cladophora-Vagabunda* (L) Vandenhoek and *Gracilaria-Tikvahiae* (Mclachlan) to environmental disturbances associated with eutrophication, *J. Exp. Mar. Biol. Ecol.*, 190, 1–16, 1995.
- Petersen, J. K., Hansen, J. W., Laursen, M. B., Clausen, P., Carstensen, J., and Conley, D. J.: Regime shift in a coastal marine ecosystem, *Ecol. Appl.*, 18, 497–510, 2008.
- Regnier, P., Wollast, R., and Steefel, C. I.: Long-term fluxes of reactive species in macrotidal estuaries: Estimates from a fully transient, multicomponent reaction-transport model, *Mar. Chem.*, 58, 127–145, 1997.
- Scheffer, M. and Carpenter, S.: Catastrophic regime shifts in ecosystems: linking theory to observation, *Trends Ecol. Evol.*, 18, 648–656, 2003.
- Scheffer, M., Carpenter, S., Foley, J. A., Folke, C., and Walker, B.: Catastrophic shifts in ecosystems, *Nature*, 413, 591–596, 2001.
- Schroder, A., Persson, L., and De Roos, A.: Direct experimental evidence for alternative stable states: a review, *Oikos*, 110, 3–19, 2005.
- Schuchardt, B., Haesloop, U., and Schirmer, M.: The tidal freshwater reach of the Weser estuary: Riverine or estuarine?, *Aquat. Ecol.*, 27, 215–226, 1993.
- Smith, V. H.: Eutrophication of freshwater and coastal marine ecosystems – A global problem, *Environ. Sci. Pollut. R.*, 10, 126–139, 2003.
- Smith, V. H.: Responses of estuarine and coastal marine phytoplankton to nitrogen and phosphorus enrichment, *Limnol. Oceanogr.*, 51, 377–384, 2006.
- Soetaert, K. and Herman, P.: Carbon flows in the Westerschelde estuary (The Netherlands) evaluated by means of an ecosystem model (MOSES), *Hydrobiologia*, 311, 247–266, 1995a.
- Soetaert, K. and Herman, P.: Nitrogen dynamics in the Westerschelde estuary (SW Netherlands) estimated by means of the ecosystem model MOSES, *Hydrobiologia*, 311, 225–246, 1995b.
- Soetaert, K. and Herman, P. M.: A practical guide to Ecological Modelling. Using R as a Simulation Platform, Springer, 2009.
- Soetaert, K., Middelburg, J., Heip, C., Meire, P., Van Damme, S., and Maris, T.: Long-term change in dissolved inorganic nutrients in the heterotrophic Scheldt estuary (Belgium, The Netherlands), *Limnol. Oceanogr.*, 51, 409–423, 2006.
- Somville, M.: Use Of Nitrifying Activity Measurements For Describing The Effect Of Salinity On Nitrification In The Scheldt Estuary, *Appl. Environ. Microb.*, 47, 424–426, 1984.
- Strayer, D. L., Pace, M. L., Caraco, N. F., Cole, J. J., and Findlay, S. E. G.: Hydrology and grazing jointly control a large-river food web, *Ecology*, 89, 12–18, 2008.
- Sundby, C. and Schiött, T.: Characterization of the reversible state of photoinhibition occurring in vitro under anaerobic conditions, *Photosynth. Res.*, 33, 195–202, 1992.
- Tackx, M., Azemar, F., Bouletreau, S., De Pauw, N., Bakker, K., Sautour, B., Gasparini, S., Soetaert, K., Van Damme, S., and Meire, P.: Zooplankton in the Schelde estuary, Belgium and the Netherlands: long-term trends in spring populations, *Hydrobiologia*, 540, 275–278, 2005.
- Tang, J. X., Hoagland, K. D., and Siegfried, B. D.: Differential toxicity of atrazine to selected freshwater algae, *B. Environ. Contam. Tox.*, 59, 631–637, 1997.
- Thomas, W. H., Hastings, J., and Fujita, M.: Ammonium Input To The Sea Via Large Sewage Outfalls. 2. Effects Of Ammonium On Growth And Photosynthesis Of Southern-California Phytoplankton Cultures, *Mar. Environ. Res.*, 3, 291–296, 1980.
- Tyystjaervi, E.: Photoinhibition of Photosystem II and photodamage of the oxygen evolving manganese cluster, *Coordin. Chem. Rev.*, 252, 361–376, 2008.
- Van Damme, S., Struyf, E., Maris, T., Ysebaert, T., Dehairs, F., Tackx, M., Heip, C., and Meire, P.: Spatial and temporal patterns of water quality along the estuarine salinity gradient of the Scheldt estuary (Belgium and The Netherlands): results of an integrated monitoring approach, *Hydrobiologia*, 540, 29–45, 2005.
- Vanderborght, J., Wollast, R., Loijens, M., and Regnier, P.: Ap-

- plication of a transport-reaction model to the estimation of biogas fluxes in the Scheldt estuary, *Biogeochemistry*, 59, 207–237, 2002.
- Vanderborght, J. P., Folmer, I. M., Aguilera, D. R., Uhrenholdt, T., and Regnier, P.: Reactive-transport modelling of C,N, and O<sub>2</sub> in a river-estuarine-coastal zone system: Application to the Scheldt estuary, *Mar. Chem.*, 106, 92–110, 2007.
- Vandijk, G., Vanliere, L., Admiraal, W., Bannink, B., and Cappon, J.: Present State Of The Water-Quality Of European Rivers And Implications For Management, *Sci. Total Environ.*, 145, 187–195, 1994.
- Wollast, R.: The Scheldt estuary, in: *Pollution of the North-Sea: an assessment*, edited by: Salomon, W., Bayne, W., Duursma, E., and Forstner, U., Springer-Verlag, Berlin, 183–193, 1988.
- Wu, R. S. S.: Hypoxia: from molecular responses to ecosystem responses, *Mar. Pollut. Bull.*, 45, 35–45, 2002.